

Spiropyran polymeric micro-capillary coatings for photo-detection of solvent polarity

*Larisa Florea,¹ Aoife McKeon,¹ Dermot Diamond,¹ Fernando Benito-Lopez *^{1,2}*

¹CLARITY: Centre for Sensor Web Technologies, National Centre for Sensor Research, Dublin City University, Dublin, Ireland, Fax: +353 1 700 7995, Tel: +353 1 700 7603

²CIC MicroGUNE, Microtechnologies Cooperative Research Center, Arrasate-Mondragón, Spain, Tel.: +34 943710212

KEYWORDS: Optical sensor, spiropyran, micro-capillary, continuous flow, solvent sensing;

ABSTRACT: Fused silica micro-capillaries were functionalised with spiropyran-polymer brushes using surface-initiated ring-opening metathesis polymerisation. Based on the inherited spiropyran properties, the functionalised capillaries were successfully used to photo-identify solvents of different polarity when passing through the micro-capillary in continuous flow. In the present study, six different solvents (toluene, tetrahydrofuran, acetone, acetonitrile, ethanol and methanol) can be easily detected while passing through the modified micro-capillary by simply irradiating a portion of it with UV light (365 nm). This converts the closed spiropyran moiety to the open merocyanine form and as a consequence, the micro-capillary gains a distinct colour and spectral response depending on the polarity of the solvent. The rate of ring opening of the spiropyran-polymer brushes coatings has been determined in-situ in the presence of different

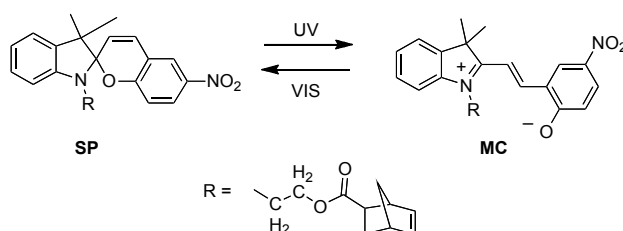
solvents, showing that the coloration rate is also influenced by the solvent polarity and therefore can be used as an additional parameter for solvent sensing.

INTRODUCTION

Optical chemical sensors for liquid phase monitoring (overwhelmingly focused on water-based samples) often employ a dye or indicator that is immobilised onto a solid support material¹⁻³. However, this strategy presents two main disadvantages: firstly, the immobilisation process may lead to losses in dye sensitivity⁴ and secondly, the stability of the sensor is affected by dye leaching into the sample solution over time³, making long-term sensor utilisation impractical. Therefore, effective optical-chemical sensors require new materials capable of overcoming all these limitations. In this context, inclusion of photochromic molecules in solid matrices is of particular interest for the development of new approaches for opto-sensing.

Since their discovery by Fisher and Hirshberg in 1952⁵, spiropyrans have become one of the most popular class of photochromic compounds in science due to their potential applicability in new technologies like data recording and storage, optical switching displays and nonlinear optics⁶⁻¹³. Spiropyrans offer new routes for the fabrication of multifunctional materials since it is possible to take advantage of their photo-reversible interconversion between the two thermodynamically stable states of the molecule: a spiropyran (SP) form, and a merocyanine (MC) form, which have dramatically different charge, polarity and molecular conformations¹⁴. The photo-chromic reaction, illustrated in Scheme 1, occurs because of the photo-cleavage of the C–O spiro-bond of the colourless SP upon UV irradiation. This yields the coloured MC isomer that can return to the SP form by ring closing under visible light irradiation or in the dark through thermal relaxation^{7, 15}. Despite the potential applications of photochromic spiropyrans, earlier studies mainly focused on evaluating the utility of monomeric SP systems in solution¹⁶⁻¹⁸.

However, more recently, researchers have tried to use spiropyran for the functionalisation of different types of surfaces. Rosario *et al.*¹⁹ coated capillary tubes with a photoresponsive monolayer based on spiropyran for photo-modulation of surface wettability. Previous work by our group showed that micro-fluidic channels coated with spiropyran monolayers can be used as photonically controlled self-indicating systems for metal ion accumulation and release, based on the metal ion-binding and molecular recognition properties which are only manifested by the MC form²⁰.



Scheme 1. Photochromic behaviour of monomeric spiropyrans.

It is well-known that the open-chain merocyanine isomers of nitro-substituted spiropyran derivatives present negative solvatochromism, meaning that their absorption bands undergo a hypsochromic (blue) shift in solvents of increasing polarity.²¹ These changes are caused by intermolecular interactions between the solute and solvent that modify the energy gap between the ground and excited states of the absorbing MC species.²² Depending on the solvent polarity, the MC form has a tendency to prevail in one of several molecular structures: neutral, cyanine-like, and charge-separated zwitterionic.²³ Based on this property, the MC isomer in solution has been studied for its potential use as an empirical indicator of solvent polarity of typical organic solvents^{24, 25}, aqueous binary solvent mixtures²⁶ and even ionic liquids.^{27, 28} Monolayers of spiropyran derivatives have been also bound to glass slides to study the polarity of their microenvironment²⁹. Although this approach offers interesting information about the interaction

of the surface-bound spiropyran with its immediate environment, it is unpractical for studying solvent polarity of a system as a whole. This is because in the monolayer approach only low-resolution fluorescence spectra can be obtained, as the surface concentration of spiropyran molecules tends to be below the detection limit of typical single-pass absorption spectrophotometers.

In this paper, we present the development of miniaturised analytical platforms wherein solvent polarity can be externally photo-detected in a completely non-invasive manner, through the employment of the colour dependency of the MC form on the solvent polarity. Functionalisation of the inner wall of a fused silica micro-capillary with this photo-responsive molecule provides an excellent platform for rapid analysis and detection of the polarity of solvents. Immobilisation of solvatochromic moieties inside flow-through units (like a micro-capillary) produces a greatly simplified and flexible platform for achieving these measurements in terms of instrumentation, operational characteristics and reagent/sample handling.³⁰

Moreover, micro-capillary platforms possess several additional attractive features such as:

- (a) They can act as a mechanical support for optically sensitive materials (coatings)³¹;
- (b) They represent an optical waveguide structure and enable various methods of optical interrogation to be employed;
- (c) They are suitable for real-time continuous flow measurements;
- (d) They require very small volumes of analyte¹ and
- (e) They can be easily integrated within commercially available systems (*e.g.* High-performance liquid chromatography (HPLC), capillary electrophoresis (CE), continuous flow and micro-fluidic devices, among others).

In order to assure a high loading of spiropyran, the coating of the capillaries was achieved via photochromic polymer brushes containing the spiropyran moiety. Although several photochromic polymers that incorporate spiropyran or other photochromic derivatives have been reported previously, such systems typically comprise polymer matrices that are either doped or side-chain-modified with photochromes in order to manifest the photochromic behaviour.³²⁻³⁴ Consequently, the total concentration of photochromic moieties tends to be low in the polymer and consequently the photochromic response is rather weak. In contrast, the micro-capillary coatings presented here are comprised of homopolymeric brushes prepared via surface-initiated ring-opening metathesis polymerisation (SI-ROMP) of a norbornyl functionalised spiropyran monomer (SP-R - Scheme 1). This approach offers a transition from a two-dimensional to a three-dimensional arrangement, which enables high surface loadings of the stimuli-responsive polymer in a limited area while maintaining the flexibility required for efficient switching of the spiropyran moiety, due to the rather open structure of the brushes which provide very high surface area to bulk characteristics.

MATERIALS AND METHODS

Reagents. 7-Octenyltrichlorosilane (Gelest), 5-norbornene-2-carboxylic acid, *exo*- (Sigma-Aldrich), 1-(2-Hydroxyethyl)-3,3-dimethylindolino-6'-nitrobenzopyrylospiran (SP1) (TCI Europe), *N,N'*-Dicyclohexylcarbodiimide (DCC) (Sigma-Aldrich), 4-(Dimethylamino)pyridine (DMAP) (Sigma-Aldrich) and Grubbs Generation-II catalyst (Sigma-Aldrich) were used as received. For the SP-R and poly(SP-R) synthesis, dry tetrahydrofuran and dry dichloromethane solvents were purchased from Sigma-Aldrich and used as received. Fused-silica micro-capillaries (100 μm ID, 375 μm OD) were purchased from Polymicro Technologies (Phoenix,

AZ, USA). The solvents used for the photo-chromic analyses - toluene, tetrahydrofuran (THF), acetone, acetonitrile (ACN), ethanol (EtOH) and methanol (MeOH), were Sigma-Aldrich HPLC grade, and used without further purification.

Synthesis of spiropyran functionalised norbornene monomer (SP-R). The monomer (SP-R) was prepared from the reaction of *exo*-5-norbornyl carboxylic acid with SP1 in the presence of *N,N'*-Dicyclohexylcarbodiimide (DCC) and 4-(Dimethylamino) pyridine (DMAP)³⁵ as described elsewhere^{35,36}. ¹H NMR (300 MHz, CDCl₃) δ (ppm): 8.05 – 8.01 (m, 2H); 7.22 (t, 1H); 7.12 (d, 1H); 6.94 - 6.90 (m, 2H); 6.78 - 6.76 (d, 1H); 6.73 - 6.71 (d, 1H); 6.15 - 6.14 (m, 1H); 6.09 - 6.06 (m, 1H); 5.93 - 5.90 (d, 1H); 4.32 - 4.11 (m, 2H); 3.57 - 3.39 (m, 2H); 3.00 - 2.91 (m, 2H); 2.19 (s, 1H); 2.19-2.14 (m, 1H); 1.90-1.83 (m, 1H); 1.49 - 1.45 (m, 1H); 1.35 (m, 1H); 1.30 (s, 3H); 1.18 (s, 3H).

Synthesis of spiropyran polymeric brushes (poly(SP-R)). Si-ROMP was performed using a modified version of the previously described method.³⁶ Briefly, prior to functionalisation, the inner surface of the fused-silica micro-capillaries was first activated with 7-octenyl trichlorosilane. The inner capillary surface (internal diameter of 100 μm and 15 cm length) was quickly washed with acetone and water, then flushed with a solution of 0.2 M NaOH for 30 min at a flow rate of 0.25 μL min⁻¹ using a syringe pump, and then rinsed with deionised water for 5 times. Next, the micro-capillary was flushed with a solution of 0.2 M HCl for 30 min at a flow rate of 0.25 μL min⁻¹, rinsed with water, dry toluene and dried under a N₂ stream. A 0.1 M solution of the silane (7-octenyl trichlorosilane) in dry toluene was pumped through the micro-capillary for 90 min at a flow rate of 0.25 μL min⁻¹. The micro-capillary was then washed with acetone, dried under a nitrogen stream, and left at room temperature for 24 h. Later, the micro-capillary was filled with a 0.02 M solution of Grubbs Catalyst Second Generation in degassed

CH₂Cl₂, closed at both ends and put in a water bath for 1 h at 45 °C. After this, the catalyst-attached micro-capillary was thoroughly washed with degassed DCM. Finally, the micro-capillary was exposed to the spiropyran functionalised monomer, SP-R (0.5 M in degassed DCM) at 50 °C for 1 h. The polymerisation was quenched by passing ethyl vinyl ether into the micro-capillary and finally, it was thoroughly washed with acetone to remove any physisorbed materials.

Characterisation. UV–vis spectroscopy for the SP-R solutions in different solvents as well as the kinetic studies of the opening process (SP-R → MC-R) were performed using a Cary 50 spectrophotometer (Varian). Morphological studies of poly (SP-R) brushes inside the micro-capillary were performed using scanning electron microscopy (SEM) on a Carl Zeiss EVOLS 15 system at an accelerating voltage of 4.27 kV. The micro-capillaries were cut using a SGT capillary column cutter with rotating diamond blade (Shortix, Nederland) to create a smooth cut of the capillary wall. Then they were placed in vertical position in a custom made metallic capillary holder that has holes of internal diameters equal to the external diameter of the micro-capillary (375 μm). This set-up allows the micro-capillaries to be kept in vertical position. During the imaging process, the stage was tilted of an angle between 0 – 15 ° for better imaging of the inner wall of the micro-capillary. Microscopy images of the micro-capillaries were performed on an Aigo digital microscope (The Dolomite Centre Ltd) equipped with a 9X auxiliary objective to give 540X total.

Light Source. Photo-conversion of the monomer solutions from SP-R to MC-R was achieved using an in-house fabricated UV light source consisting of three UV LEDs (Roithner LaserTechnik GmbH, emission $\lambda_{\text{max}} = 375 \text{ nm}$). The vials were placed 2 cm from the source and irradiated at a power of 0.4 mW cm⁻² for 20 s using a 3.75 V supply. The white light irradiation

was provided via a LMI-6000 LED Fiber Optic Illuminator obtained from Dolan-Jenner Industries and was used to switch the MC-R monomer solutions and the poly(MC-R) coatings, back to the closed SP-R and poly(SP-R) form, respectively. Also in this case, the vials/capillaries were placed at 2 cm from the light source and were irradiated for 20 s. The maximum light output of the lamp is 780 Lumens, and the intensity control of the light output was fixed at 50 %.

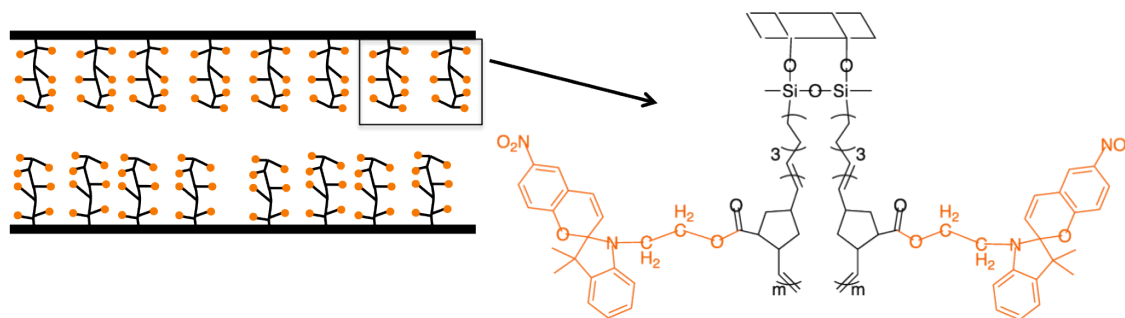
Photochemical Methods. UV-Vis Spectroscopy was used to study the solvent dependence of the poly(SP-R) coatings while different solvents were passed through the modified micro-capillary in continuous flow. The absorbance spectra were recorded using two fiber-optic light guides connected to a Miniature Fiber Optic Spectrometer (USB4000 - Ocean Optics) and aligned using a cross-shaped cell (ESI - Scheme S1). The light source used was a DH-2000-92 BAL UV-NIR deuterium tungsten halogen source (Ocean Optics). The six solvents (toluene, tetrahydrofuran, acetone, acetonitrile, ethanol and methanol, respectively) were passed through the micro-capillary at a constant flow rate of $0.5 \mu\text{L min}^{-1}$ using a syringe pump (PHD 2000 Syringe, Harvard Apparatus). Individual absorbance spectra were recorded in-situ after 60 s of irradiation while the kinetics curves for the ring-opening process were obtained by continuously monitoring the absorbance value (acquisition interval of 2 s) for each of the solvents at their characteristic maximum wavelength (λ_{max}) for 190 s, until the absorbance reaches a plateau. The data from the spectrometer were processed using Spectrasuite software provided by Ocean Optics Inc. For better clarity, each recorder absorbance spectra was smoothed using Origin software via the Savitzky-Golay algorithm. A single exponential model (eqn. (1)) was used to determine the ring opening rate constant for the SP-R monomer (see ESI) and the poly(SP-R) coatings.

$$y = a (1 - e^{-(kt)}) + b \quad (1)$$

where y is the absorbance at λ_{\max} (assumed to be proportional to the concentration of the merocyanine isomer), a is a scaling factor, k is the first order rate constant (s^{-1}), b is the baseline offset and t is time (s).

RESULTS AND DISCUSSION

(SP-R) polymeric coatings. Surface-initiated ring-opening metathesis polymerisation (SI-ROMP) of spirocyan norbornene monomers catalysed by Grubbs Catalyst Second Generation has proven to be an efficient method to grow polymer brushes from surfaces³⁷ and micro-capillaries³⁶. This polymerisation technique, allows a 3D arrangement of polymer brushes to be obtained (Scheme 2), which is very desirable when building micro-capillary-integrated optical sensors, as high concentrations of the sensing unit are necessary to compensate for the micrometre size path length.



Scheme 2. Representation of the fused silica micro-capillary functionalised with spirocyan polymeric brushes.

Clear improvements have been obtained when comparing with the previously reported method published by us³⁶, in the case of poly(SP-R) micro-capillary coatings, by using *exo*-norbornene carboxylic acid as the starting material for the production of the spirocyan *exo*-norbornene monomer (SP-R), instead of a mixture of *exo*- and *endo*- isomers. Several reports on the ROMP

of other norbornene derivatives have shown that *exo*- isomers often react faster than the corresponding *endo*- one. The steric interactions between the growing polymer chain and the incoming monomers appear to be the primary cause of this reactivity difference³⁸. The time for polymerisation was fixed to one hour. These new conditions allowed better control over the grafting density and therefore more homogenous coatings were obtained along the entire length of the micro-capillary (contrary to the previously reported method). Scanning electron microscopy of the inner wall of the micro-capillary showed a 3D arrangement of the polymer brushes with a thickness of about 2-3 μm as shown in Figure 1, thicker than in the previously reported method (1 -2 μm). These results show that by using only the *exo*- isomer of SP-R, both coating homogeneity and thickness are greatly improved while the polymerisation time is reduced to one hour.

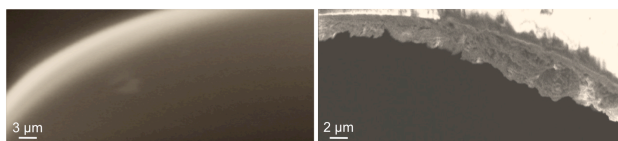


Figure 1. Scanning Electron Microscopy (SEM) images of the inner wall of a fused silica micro-capillary before (left) and after (right) functionalisation with spiropyran polymeric brushes.

Solvent sensing. The solvatochromic properties of SP-R monomer and poly(SP-R) brushes were tested using six solvents of differing polarities: toluene (relative polarity ($p'=0.099$))²², THF ($p'=0.207$)²², acetone ($p'=0.355$)²², ACN ($p'=0.460$)²², EtOH ($p'=0.654$)²² and MeOH ($p'=0.762$)²².

As previously described, the coloured MC form is well known to undergo solvatochromism^{21, 29, 39, 40}. Solvatochromism refers to a strong dependence of the UV-vis absorption bands of a

compound on the polarity of the solvent medium. This typically manifests as changes in the position, and intensity of the absorption bands of the molecule when measured in different solvents. These changes are caused by intermolecular interactions between the solute and the solvent, modifying the energy gap between the ground and excited state of the absorbing species. The colour of the MC form depends on the difference in polarity between the photo-excited MC form and the conjugated zwitterionic ground state. The coloured MC form is highly conjugated and characterised by a strong polar character, due to its zwitterionic structure, which strongly contributes to the electronic distribution of the ground state. As a consequence, the ground state of the MC form is stabilised in polar solvents relative to the excited state, leading to larger energy gap than in non-polar solvents. In non-polar solvents, the energy difference between the ground and the excited state is much lower, because of the high energy level of the ground state. As a result, as the polarity of the solvent increases, the maximum absorbance shifts to shorter wavelengths, higher frequency (hypsochromic or blue shift), while as the polarity decreases the maximum absorbance shifts to longer wavelengths, lower frequency (bathochromic or red shift). When, for instance, a solution of SP-R (10^{-3} M) is irradiated with UV light in MeOH, EtOH, ACN, acetone, THF and toluene (Figure 2), the solution shows a strong colour change – from pink to blue. This colour disappears after irradiation of the solution with white light, since the MC form reverts to the non-solvatochromic SP form, and the solution becomes colourless. This behaviour shows that the SP-R monomer inherits the photochromic and solvatochromic properties of the reactant SP1, well known for its solvatochromic properties.^{21, 29, 39, 40}

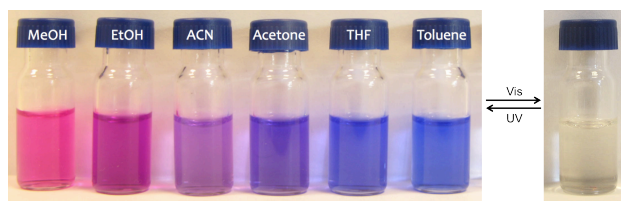


Figure 2. Pictures of six vials (left) containing a solution of the SP-R monomer (10^{-3} M) when irradiated for 20 seconds with UV light in different solvents and after irradiation with white light for 20 s (right).

As seen from Figure 3, the absorbance spectra of the monomer open form (MC-R) shows that the λ_{\max} of MC-R undergoes red and blue shifts depending on the solvent polarity. Among the solvents analysed, the lowest λ_{\max} value was found in the presence of MeOH (540 nm). This value increases to 552 nm in EtOH, 568 nm in ACN, and 574 nm in acetone, which indicates a significantly more non-polar environment. The highest values are observed for THF (587 nm) and toluene (609 nm) (Figure 3). In the absorbance spectra of the MC-R in toluene a shoulder around 565 nm is clearly defined. This can be attributed to the presence of MC aggregates which are known to form in certain non-polar solvents under UV-irradiation.^{7,41} In general two types of aggregates have been identified: *J*-aggregates which have parallel arrangement and present a shift to longer wavelengths, while *H*-aggregates have a head to tail arrangement of the MC dipoles and the spectra are shifted to shorter wavelengths.⁵

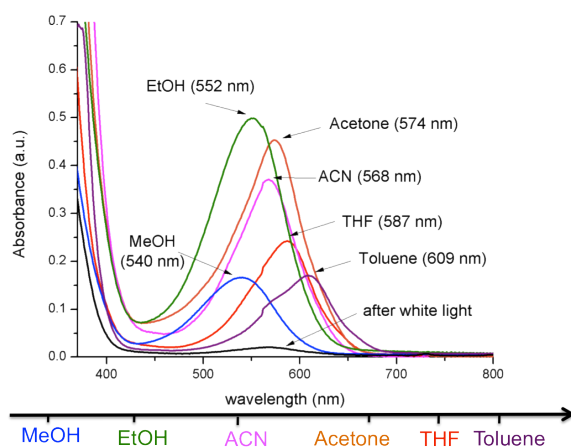


Figure 3. Absorption spectra of the SP-R monomer (10^{-3} M) solution in MeOH, EtOH, ACN, acetone, THF and toluene after UV and white light irradiation.

Analysing the absorbance shifts presented by the MC-R isomer in the six different solvents, it was observed that they are in perfect agreement with the Reichardt's empirical $E_T(30)$ polarity scale described in the "Solvents and Solvent Effects in Organic Chemistry".²² This scale is based on the solvent-dependent spectral shifts experienced by pyridinium *N*-phenoxide betaine dye $E_T(30)$ and has been shown to take into consideration both the polarity and the hydrogen bond donating acidity of the solvent.²² The absorption λ_{\max} of the MC-R in different solvents was found to give good linear correlations with the normalised $E_T(30)$ ($R^2 = 0.97$), similarly with other reported spiropyran derivatives²⁹ (Figure 4). Good correlation between the solvatochromic behaviours of the two was expected as both merocyanines and $E_T(30)$ are meropolymethines dyes. The negative slopes of the plots indicate that in polar solvents, the ground state of the MC form is stabilised relatively to the excited state (lower wavelengths means larger energy gap between the ground and excited state) while the linear fit implies that there is a hydrogen bond contribution to this effect.²⁹

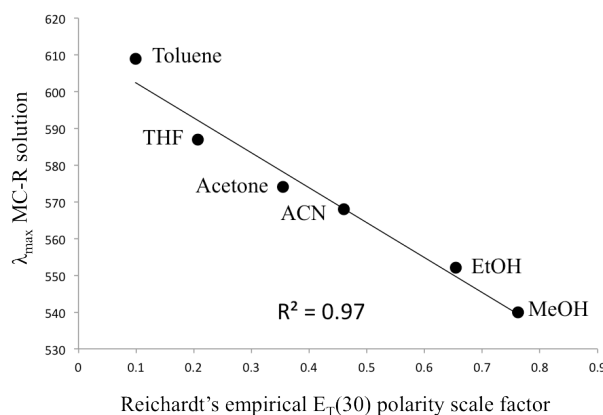


Figure 4. Linear correlation between Reichardt's empirical $E_T(30)$ polarity scale factor and the absorption λ_{\max} of SP-R monomeric solutions (10^{-3} M) in different solvents.

When the six different solvents are passed through the micro-capillary functionalised with SP-R polymeric brushes at a flow rate of $0.5 \mu\text{L min}^{-1}$ followed by the exposure of the micro-capillary to UV light (20 s), the colour of the micro-capillary changes according to the polarity of the solvent, from red (highly polar) towards blue (highly non-polar), following a similar behaviour to the SP-R monomer solutions (Figure 5). Moreover, when the micro-capillary is exposed to white light irradiation (20 s), it returns to the initial colourless spiropyran form, Figure 5-bottom. This demonstrates that in the polymer brush structures, which are densely packed with spiropyran moieties, there is no evidence of steric hindrance of the characteristic SP to MC photo-switching in response to UV and white light irradiation, and that the merocyanine unit maintains its solvatochromic properties intact.

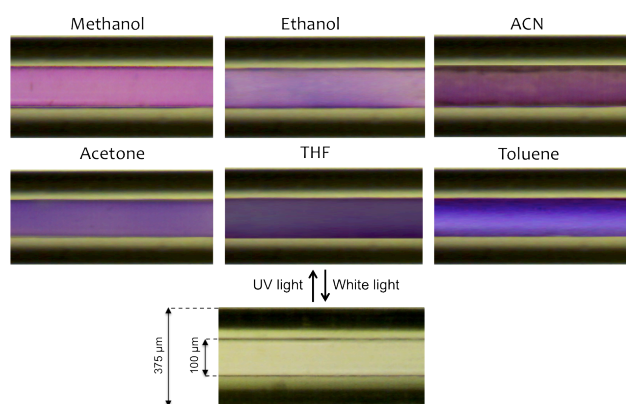


Figure 5. Pictures of the poly(SP-R) coated micro-capillary when irradiated for 20 s with UV light while different solvents are passed through the micro-capillary in continuous flow ($0.5 \mu\text{L min}^{-1}$) and after irradiation with white light for 20 s.

UV-vis spectra of the polymer brushes were taken using the set-up described in the ESI, Scheme S1, permitting *in situ* spectroscopic characterisation of the coatings inside the micro-capillary. When in the merocyanine form, the polymer coatings show an absorbance band with a λ_{max} of 558 nm when the solvent is MeOH, 565 nm in the case of EtOH, 567 nm for ACN, 571

nm for acetone, 575 nm for THF and 576 nm for toluene, respectively (Figure 6). Therefore, the poly(SP-R) coatings indicate negative solvatochromism, similar to that shown by the SP-R monomer in solution. These absorption bands disappear after irradiation of the micro-capillary with white light for 20 s due to interconversion to the non-solvatochromic spiropyran form. This process is completely reversible, implying that the platform can be switched between sensing and non-sensing modes entirely using light.³⁶ The shift of the λ_{max} in the absorption spectra of the polymer brushes compared to that of the monomer in solution is most likely due to the local environmental effects that are related to the immobilisation of the spiropyran moiety⁴² and to the swelling effect of the polymer brushed when in presence of different solvents.⁴³ It can be explained taking into account the compact organisation of spiropyran units in the polymer brushes, wherein the conformation of a single spiropyran moiety is not only influenced by the solvent but also by the neighbouring spiropyran units that may be present in their polar merocyanine form. The lower dynamic range of the λ_{max} in the case of polymeric brushes compared with the SP in solution is most probably due to the architecture of the coating and can be explained by taking into consideration two factors: the much higher concentration of spiropyran units inside the polymeric brushes compared with the solution as well as steric hindrances inside the coating, that restricts the conformational freedom of the spiropyran moiety. Nevertheless, the shifts in the absorption λ_{max} of the poly(SP-R) coatings are also, in this case, in good agreement with the Reichardt's empirical $E_{\text{T}}(30)$ polarity scale, showing reasonably good linear correlations between the absorption λ_{max} of the poly(SP-R) coatings and the normalised $E_{\text{T}}(30)$, just like in the case of SP-R solutions ($R^2 > 0.95$) (Figure 7).

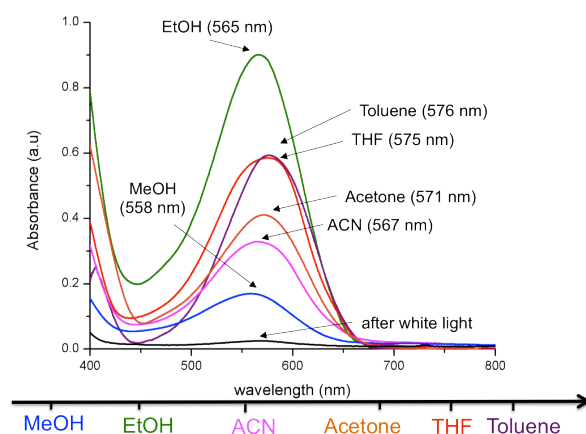


Figure 6. Absorption spectra of the poly(SP-R) functionalised capillary when MeOH, EtOH, ACN, acetone, THF and toluene, respectively are passed through the micro-capillary, after UV and white light irradiation.

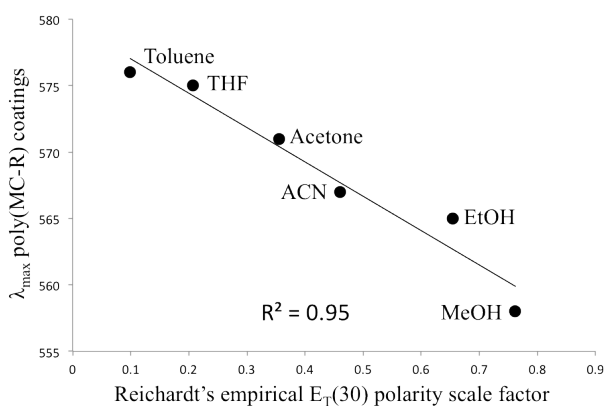


Figure 7. Linear correlation between Reichardt's empirical $E_T(30)$ polarity scale factor and the absorption λ_{\max} of poly(SP-R) coatings in the presence of different solvents.

These results indicate that poly(SP-R) coated micro-capillary could be used for the detection of solvents of different polarities based on the colour (absorption λ_{\max}) of the micro-capillary after UV irradiation. This is the first time such a micro-capillary integrated polarity sensor has been reported, capable of performing in continuous flow mode. Moreover, this sensing behaviour can be switched on/off remotely by using light, either along the entire length of the micro-capillary,

or at patterned locations using appropriate masks³⁶. In addition, these colour changes could be easily quantified using digital image processing techniques^{44,45}, or by simple visual observation.

Kinetics of photo-induced ring opening. As the system described in Scheme S1 (ESI) allows in-situ monitoring of the ring opening process of the poly(SP-R) coatings, kinetic studies were performed in order to evaluate how the different solvents may affect the ring opening kinetics of the poly(SP-R) and so, provide an additional parameter for solvent sensing. This involved, inducing the formation of the poly(MC-R) state by continuous exposure of the micro-capillary to UV light and recording the absorbance value of the MC-R, at the corresponding λ_{max} in each solvent at fixed time intervals (1 s), until the absorbance value reaches a plateau (approximately 180 s). During these measurements, the micro-capillary is kept in a fixed position, in the dark, inside the cross-shaped detection cell as shown in Scheme S1 (ESI) in order to avoid the influence of the ambient light.

The λ_{max} absorbance values in each solvent were obtained from Figure 6 and modelled according to eqn. (1). Figure 8 shows the absorbance increase over time at the λ_{max} (293 K) for each of the solvents (MeOH, EtOH, ACN, acetone, THF and toluene, respectively) for the poly(SP-R) coating, using the first-order kinetics model.⁴⁶ The first-order rate constants were estimated by fitting the absorbance values at λ_{max} using Microsoft Excel Solver and eqn.(1). All the ring-opening kinetics were estimated in triplicate, and at different locations on the micro-capillary, for all the six solvents, showing great reproducibility (See ESI – Figure S1). Moreover, the fact that the absorbance at λ_{max} stabilises at the same absorbance values in different positions on the micro-capillary for each individual solvent, demonstrates the excellent homogeneity of the coatings.

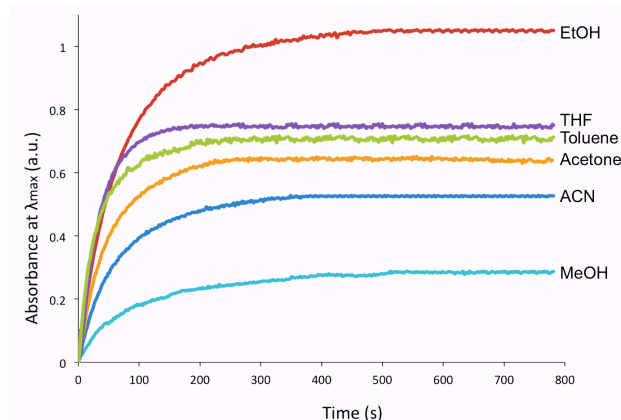


Figure 8. Ring opening kinetics of the spiropyran polymeric coatings in different solvents showing the conversion of poly(SP-R) to poly(MC-R). The values of the absorbance were taken at $\lambda_{\max} = 558$ nm for MeOH, $\lambda_{\max} = 565$ nm for EtOH, $\lambda_{\max} = 567$ nm for ACN, $\lambda_{\max} = 571$ nm for acetone, $\lambda_{\max} = 575$ nm for THF and $\lambda_{\max} = 576$ nm for toluene at 293 K.

The ring opening process analysed using eqn. (1) occurs about 1.3 times faster for EtOH compared to MeOH and about 1.5 times faster for ACN and acetone compared to MeOH. The fastest ring-opening kinetics were obtained for THF and toluene at about 2.7 and 2.8 times faster, respectively, than in MeOH. Under these conditions, the ring opening kinetics of poly(SP-R) show that for poly(MC-R) formation in toluene, the steady-state (ca. 0.7 a.u.) is reached in about 200 s while for the formation of poly(MC-R) steady-state in Acetone and ACN, the absorbance becomes relatively constant at ca. 0.6 a.u. and 0.5 a.u. after about 300 and 400 s, respectively. This may be due to the faster ring-opening rate obtained in non-polar solvents compared to polar solvents. Although the influence of the solvent on the ring-opening kinetics has been considered to be weak³⁹, in the present circumstances, the pattern that emerges is clear and convincing: as the polarity of the solvent decreases the rate of the ring opening process increases. A possible explanation for this behaviour lies in the mechanism of the ring-opening of the spiropyran

moiety itself. The interconversion between SP and MC involves an intermediate, which is formed as the bond between the spiro carbon atom and the pyran oxygen atom is ruptured while the orthogonal topology is retained. As shown before, this step is the rate-determining step in the coloration reaction (SP to MC).⁴⁰ As the intermediate, a *cis-cisoid* isomer of MC, has a non-polar character, it is expected to be stabilised in less polar solvents causing faster ring-opening kinetics in solvents of decreasing polarity. Further indications supporting this statement have been found by comparing the ring opening kinetics of poly(SP-R) coatings with the ring opening kinetics of SP-R in solution (See ESI – Figure S2). The ring-opening process in solution also followed first order kinetics, and therefore the first-order rate constants were estimated by fitting the absorbance values at λ_{max} using Microsoft Excel Solver via eqn. (1) (See ESI – Figure S3). The results obtained for the SP-R in solution are in close agreement with those obtained for the poly(SP-R) coatings, reinforcing the view that the ring-opening rate increases as the solvent polarity decreases (See ESI Table S1). The estimated rate of ring opening of SP-R to MC-R in solution is about 1.1 times higher for EtOH compared to MeOH and about 3 times higher for acetone compared to ACN. The fastest ring-opening kinetics were obtained for THF and toluene where the SP-R coloration occurs approximately 2.5 times faster in toluene than in THF. Table 1 lists the solvents and values of the relevant solvent polarity scales used for the analysis of the solvatochromic behavior of the poly(SP-R) coatings.

Table 1. poly(MC-R) λ_{max} values in different solvents reported together with the normalised Reichardt's empirical $E_{\text{T}}(30)$ polarity scale factor. These values are followed by the rate constants (\pm absolute error, $n = 3$), for the ring opening equilibrium obtained from the best-fit

curves of the absorbance-time curves (Figure S1, ESI) recorded at the corresponding poly(MC-R) λ_{\max} in each solvent.

Solvent	$E_T(30)$	λ_{\max} (nm)	k (s ⁻¹)
Methanol	0.762	558	$1.04 \times 10^{-2} \pm 0.9 \times 10^{-3}$
Ethanol	0.654	565	$1.34 \times 10^{-2} \pm 0.3 \times 10^{-3}$
ACN	0.460	567	$1.52 \times 10^{-2} \pm 0.8 \times 10^{-3}$
Acetone	0.355	571	$1.56 \times 10^{-2} \pm 1.8 \times 10^{-3}$
THF	0.207	575	$2.73 \times 10^{-2} \pm 1.1 \times 10^{-3}$
Toluene	0.099	576	$2.84 \times 10^{-2} \pm 1.7 \times 10^{-3}$

CONCLUSIONS

Spiropyran based polymer brushes grafted onto the inner walls of a micro-capillary have been used for rapid and sensitive solvent polarity detection. The micro-capillary can be functionalised in a highly homogeneous manner along its entire length since the functionalisation is performed in a continuous flow mode. We have demonstrated the feasibility of a self-diagnosing tool for sensing based on a micro-capillary, which can be operated in continuous flow, and is capable of detecting and reporting variations in the local polarity of the medium in contact with the spiropyran polymeric coatings of the micro-capillary through changes in the surface coating. *In-situ* ring-opening kinetics of the spiropyran polymeric coatings have demonstrated highly reproducible performance of the coatings while the rate constant of the ring-opening process have been shown to be influenced by the solvent polarity and could serve as an additional parameter for solvent sensing. ROMP chemistry provides a route to the formation of rather thick, yet highly open brush-type coatings with high SP-R loading, which provide the basis for

colourimetric measurements that combine high sensitivity with rapid kinetics. The photoswitchable nature of the sensing molecule means that this function can be turned on/off in a temporal and spatially controllable manner using UV/visible light, respectively.

AUTHOR INFORMATION

Corresponding Author

*E-mail: fbenito@cicmicrogune.es and fernando.lopez@dcu.ie (Fernando Benito-Lopez);
Tel.: +34 943710212 Fax: +34 943710212 ;

ACKNOWLEDGMENT

The project has been carried out with the support of the Irish Research Council (IRC) - Embark Initiative and Science Foundation Ireland under the CLARITY award (07/CE/ I1147).

ASSOCIATED CONTENT

Supporting Information. A schematic of the set-up used for absorbance and kinetics measurements for the poly(SP-R) capillary coatings is provided (Scheme S1) as are experimental and fitted kinetic curves of the photo-induced ring opening of poly(SP-R) coatings in different solvents (Figure S1). Kinetics of photo-induced ring opening equilibrium of SP-R monomer in solution - experimental and fitted kinetic curves are given (Figures S2 and S3) along with associated values of the rate constants, for the photo-induced ring opening process of SP-R monomer solutions (10^{-3} M), in different solvents (Table S1). This material is available free of charge via the Internet at <http://pubs.acs.org>.

REFERENCES

1. Weigl, B. H.; Wolfbeis, O. S., Capillary optical sensors. *Anal. Chem.* **1994**, *66*, (20), 3323-3327.
2. Kuswandi, B.; Narayanaswamy, R., Capillary optode: Determination of mercury(II) in aqueous solution. *Anal. Lett.* **1999**, *32*, (4), 649-664.
3. Kuswandi, B.; Narayanaswamy, R., Polymeric encapsulated membrane for optodes. *Fresenius J. Anal. Chem.* **1999**, *364*, (6), 605-607.
4. Buchholz, F.; Buschmann, N.; Cammann, K., A fiberoptic sensor for the determination of sodium with a reversible response. *Sens. Actuators, B* **1992**, *9*, (1), 41-47.
5. Fischer, E.; Hirshberg, Y., Formation of coloured forms of spirans by low-temperature irradiation. *J. Chem. Soc.* **1952**, 868, 4522-4524.
6. Zhu, M. Q.; Zhu, L. Y.; Han, J. J.; Wu, W. W.; Hurst, J. K.; Li, A. D. Q., Spiropyran-based photochromic polymer nanoparticles with optically switchable luminescence. *J. Am. Chem. Soc.* **2006**, *128*, (13), 4303-4309.
7. Minkin, V. I., Photo-, thermo-, solvato-, and electrochromic spiroheterocyclic compounds. *Chem. Rev.* **2004**, *104*, (5), 2751-2776.
8. Uchida, K.; Takata, A.; Saito, M.; Murakami, A.; Nakamura, S.; Irie, M., A novel photochromic film by oxidation polymerization of a bisbenzothienylethene with phenol groups. *Adv. Mater.* **2003**, *15*, (10), 785-788.
9. Zhang, Y.; Shao, N.; Yang, R.; Li, K. a.; Liu, F.; Chan, W.; Mo, T., Utilization of a spiropyran derivative in a polymeric film optode for selective fluorescent sensing of zinc ion. *Sci. China, Ser. B* **2006**, *49*, (3), 246-255.
10. Ma, Y.; Niu, C.; Wen, Y.; Li, G.; Wang, J.; Li, H.; Du, S.; Yang, L.; Gao, H.; Song, Y., Stable and reversible optoelectrical dual-mode data storage based on a ferrocenylspiropyran molecule. *Appl. Phys. Lett.* **2009**, *95*, (18), 183307.
11. Vollmer, H. P., Investigations on quantum yield and stability of coloration of uv-sensitive spiropyran layers used as a recording material for optical data storage. *Z. Naturforsch., A: Phys. Sci.* **1975**, *30*, (11), 1425-1432.
12. Bobrovsky, A. Y.; Boiko, N. I.; Shibaev, V. P., Photosensitive cholesteric copolymers with spiropyran-containing side groups: Novel materials for optical data recording. *Adv. Mater.* **1999**, *11*, (12), 1025-1028.
13. Jiang, G.; Song, Y.; Guo, X.; Zhang, D.; Zhu, D., Organic functional molecules towards information processing and high-density information storage. *Adv. Mater.* **2008**, *20*, (15), 2888-2898.
14. Tian, H.; Feng, Y., Next step of photochromic switches? *J. Mater. Chem.* **2008**, *18*, (14), 1617-1622.
15. Hirshberg, Y., Reversible formation and eradication of colors by irradiation at low temperatures - a photochemical memory model. *J. Am. Chem. Soc.* **1956**, *78*, (10), 2304-2312.
16. Berkovic, G.; Krongauz, V.; Weiss, V., Spiroyrans and spirooxazines for memories and switches. *Chem. Rev.* **2000**, *100*, (5), 1741-1753.
17. Preigh, M. J.; Stauffer, M. T.; Lin, F. T.; Weber, S. G., Anodic oxidation mechanism of a spiropyran. *J. Chem. Soc., Faraday Trans.* **1996**, *92*, (20), 3991-3996.
18. Zhu, J.-F.; Yuan, H.; Chan, W.-H.; Lee, A. W. M., A colorimetric and fluorescent turn-on chemosensor operative in aqueous media for Zn(2+) based on a multifunctionalized spirobenzopyran derivative. *Org. Biomol. Chem.* **2010**, *8*, (17), 3957-3964.

19. Rosario, R.; Gust, D.; Hayes, M.; Jahnke, F.; Springer, J.; Garcia, A. A., Photon-modulated wettability changes on spiropyran-coated surfaces. *Langmuir* **2002**, *18*, (21), 8062-8069.
20. Benito-Lopez, F.; Scarmagnani, S.; Walsh, Z.; Paull, B.; Macka, M.; Diamond, D., Spiropyran modified micro-fluidic chip channels as photonically controlled self-indicating system for metal ion accumulation and release. *Sens. Actuators, B* **2009**, *140*, (1), 295-303.
21. Keum, S. R.; Hur, M. S.; Kazmaier, P. M.; Buncel, E., Thermochromic and photochromic dyes - indolino-benzospiropyrans .1. uv-vis spectroscopic studies of 1,3,3-spiro(2H-1-benzopyran-2,2'-indolines) and the open-chain merocyanine forms - solvatochromism and medium effects on spiro ring formation. *Can. J. Chem.* **1991**, *69*, (12), 1940-1947.
22. Reichardt, C., *Solvents and Solvent Effects in Organic Chemistry*. Fourth Edition ed.; Wiley-VCH Verlag GmbH & Co. KGaA: 2010.
23. Murugan, N. A.; Chakrabarti, S.; Agren, H., Solvent Dependence of Structure, Charge Distribution, and Absorption Spectrum in the Photochromic Merocyanine-Spiropyran Pair. *J. Phys. Chem. B* **2011**, *115*, (14), 4025-4032.
24. Botrel, A.; Aboab, B.; Corre, F.; Tonnard, F., A theoretical investigation of solvatochromism - application to merocyanines similar to colored forms obtained by flash-photolysis of spiropyranes. *Chem. Phys.* **1995**, *194*, (1), 101-116.
25. Shirinian, V. Z.; Besugliy, S. O.; Metelitsa, A. V.; Krayushkin, M. M.; Nikalin, D. M.; Minkin, V. I., Novel photochromic spirocyclic compounds of thienopyrroline series: 1 Spiropyranes. *J. Photochem. Photobiol., A* **2007**, *189*, (2-3), 161-166.
26. Keum, S.-R.; Roh, S.-J.; Ahn, S.-M.; Lim, S.-S.; Kim, S.-H.; Koh, K., Solvatochromic behavior of non-activated indolinobenzospiropyran 6-carboxylates in aqueous binary solvent mixtures. Part II. *Dyes Pigm.* **2007**, *74*, (2), 343-347.
27. Byrne, R.; Coleman, S.; Gallagher, S.; Diamond, D., Designer molecular probes for phosphonium ionic liquids. *Phys. Chem. Chem. Phys.* **2010**, *12*, (8), 1895-1904.
28. Byrne, R.; Coleman, S.; Fraser, K. J.; Raduta, A.; MacFarlane, D. R.; Diamond, D., Photochromism of nitrobenzospiropyran in phosphonium based ionic liquids. *Phys. Chem. Chem. Phys.* **2009**, *11*, (33), 7286-7291.
29. Rosario, R.; Gust, D.; Hayes, M.; Springer, J.; Garcia, A. A., Solvatochromic study of the microenvironment of surface-bound spiropyranes. *Langmuir* **2003**, *19*, (21), 8801-8806.
30. Bosch Ojeda, C.; Sanchez Rojas, F., Recent development in optical chemical sensors coupling with flow injection analysis. *Sensors* **2006**, *6*, (10), 1245-1307.
31. Florea, L.; Diamond, D.; Benito-Lopez, F., Polyaniline Coated Micro-capillaries for Continuous Flow Analysis of Aqueous Solutions. *Anal. Chim. Acta.* **2012**, doi: <http://dx.doi.org/10.1016/j.aca.2012.11.027>.
32. Gonzalez-de los Santos, E. A.; Lozano-Gonzalez, M. J.; Johnson, A. F., Photoresponsive polyurethane-acrylate block copolymers. I. Photochromic effects in copolymers containing 6'-nitro spiropyranes and 6'-nitro-bis-spiropyranes. *J. Appl. Polym. Sci.* **1999**, *71*, (2), 259-266.
33. Marsella, M. J.; Wang, Z. Q.; Mitchell, R. H., Backbone photochromic polymers containing the dimethyldihydropyrene moiety: Toward optoelectronic switches. *Org. Lett.* **2000**, *2*, (19), 2979-2982.
34. Guo, X. F.; Zhang, D.; Gui, Y.; Wax, M. X.; Li, J. C.; Liu, Y. Q.; Zhu, D. B., Reversible photoregulation of the electrical conductivity of spiropyran-doped polyaniline for information recording and nondestructive processing. *Adv. Mater.* **2004**, *16*, (7), 636-640.

35. Keum, S.-R.; Ahn, S.-M.; Roh, S.-J.; Ma, S.-Y., The synthesis and spectroscopic properties of novel, photochromic indolinobenzospiropyran-based homopolymers prepared via ring-opening metathesis polymerization. *Dyes Pigm.* **2010**, *86*, (1), 74-80.
36. Florea, L.; Hennart, A.; Diamond, D.; Benito-Lopez, F., Synthesis and characterisation of spiropyran-polymer brushes in micro-capillaries: Towards an integrated optical sensor for continuous flow analysis. *Sens. Actuators B: Chem.* **2012**, *175*, 92-99.
37. Samanta, S.; Locklin, J., Formation of photochromic spiropyran polymer brushes via surface-initiated, ring-opening metathesis polymerization: Reversible photocontrol of wetting behavior and solvent dependent morphology changes. *Langmuir* **2008**, *24*, (17), 9558-9565.
38. Rule, J. D.; Moore, J. S., ROMP reactivity of endo- and exo-dicyclopentadiene. *Macromolecules* **2002**, *35*, (21), 7878-7882.
39. Zhou, J. W.; Li, Y. T.; Tang, Y. W.; Zhao, F. Q.; Song, X. Q.; Li, E. C., Detailed investigation on a negative photochromic spiropyran. *J. Photochem. Photobiol., A* **1995**, *90*, (2-3), 117-123.
40. Song, X. Q.; Zhou, J. W.; Li, Y. T.; Tang, Y. W., Correlations between solvatochromism, Lewis acid-base equilibrium and photochromism of an indoline spiropyran. *J. Photochem. Photobiol., A* **1995**, *92*, (1-2), 99-103.
41. Uznanski, P., UV-assisted formation of nanoaggregates from photochromic spiropyrans in nonpolar solvents. *Langmuir* **2003**, *19*, (6), 1919-1922.
42. Fries, K. H.; Driskell, J. D.; Samanta, S.; Locklin, J., Spectroscopic Analysis of Metal Ion Binding in Spiropyran Containing Copolymer Thin Films. *Anal. Chem.* **2010**, *82*, (8), 3306-3314.
43. Kong, B.; Lee, J. K.; Choi, I. S., Surface-Initiated, Ring-Opening Metathesis Polymerization: Formation of Diblock Copolymer Brushes and Solvent-Dependent Morphological Changes. *Langmuir* **2007**, *23*, (10), 6761-6765.
44. Byrne, L.; Barker, J.; Pennarun-Thomas, G.; Diamond, D.; Edwards, S., Digital imaging as a detector for generic analytical measurements. *TrAC, Trends Anal. Chem.* **2000**, *19*, (8), 517-522.
45. Fay, C.; Lau, K.-T.; Beirne, S.; Conaire, C. O.; McGuinness, K.; Corcoran, B.; O'Connor, N. E.; Diamond, D.; McGovern, S.; Coleman, G.; Shepherd, R.; Alici, G.; Spinks, G.; Wallace, G., Wireless aquatic navigator for detection and analysis (WANDA). *Sens. Actuators, B* **2010**, *150*, (1), 425-435.
46. Zanoni, M.; Coleman, S.; Fraser, K. J.; Byrne, R.; Wagner, K.; Gambhir, S.; Officer, D. L.; Wallace, G. G.; Diamond, D., Physicochemical study of spiropyran-terthiophene derivatives: photochemistry and thermodynamics. *Phys. Chem. Chem. Phys.* **2012**, *14*, (25), 9112-9120.

TOC Graphic

